

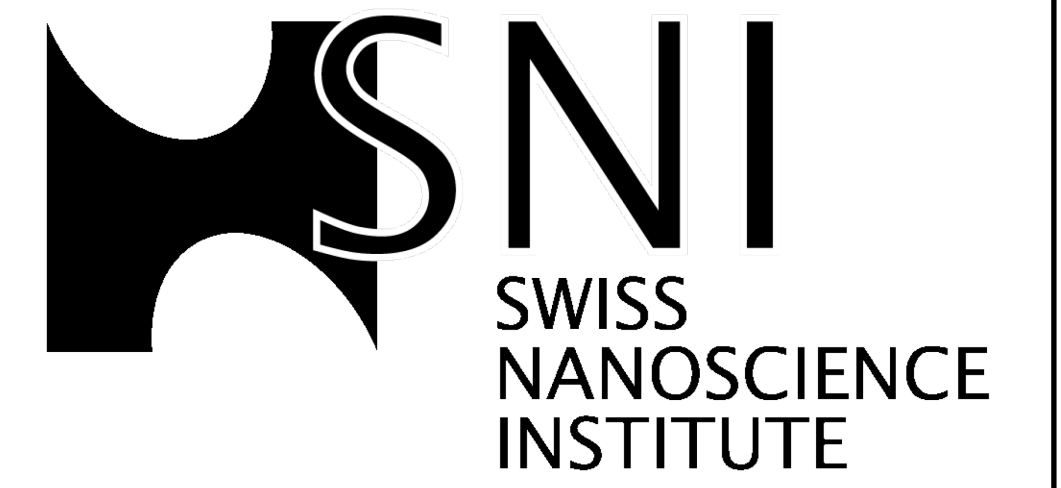
BRAF mutational analysis of malignant melanoma biopsies

F. Huber¹, H. P. Lang¹, D. Rimoldi², Ch. Gerber¹, K. Glatz³, and E. Meyer¹

¹ Swiss Nanoscience Institute, University of Basel, Klingelbergstrasse 82, CH-4056 Basel

² Ludwig Center for Cancer Research, University of Lausanne, Ch. des Boveresses 155, CH-1066 Epalinges

³ Institute for Pathology, University Hospital Basel, Schönbeinstrasse 40, CH-4031 Basel



EINE INITIATIVE DER UNIVERSITÄT BASEL UND DES KANTONS AARGAU

Abstract

We performed the first clinical pilot study based on nanomechanical microcantilever sensors demonstrating the identification of the *BRAF*^{V600E} single-point mutation in total RNA extracted from biopsies of malignant melanoma of different origins and forms (frozen or formalin-fixed paraffin-embedded tissues). The occurrence of cutaneous malignant melanoma has steadily increased over the past 50 years and continues to rise in most western countries. Malignant melanoma represents less than 5% of all skin cancers, but accounts for the majority of fatalities. Fortunately, in recent years new more efficient treatments have become available to combat the disease. Among them are highly specific inhibitors that take advantage of the presence of particular driver mutations in various genes, e.g., *BRAF*^{V600E}. An important task is to identify the patients who have this mutation and therefore can profit from the treatment. The work presented here shows a method to detect the mutation in total RNA from biopsies and does not rely on amplification or labeling.

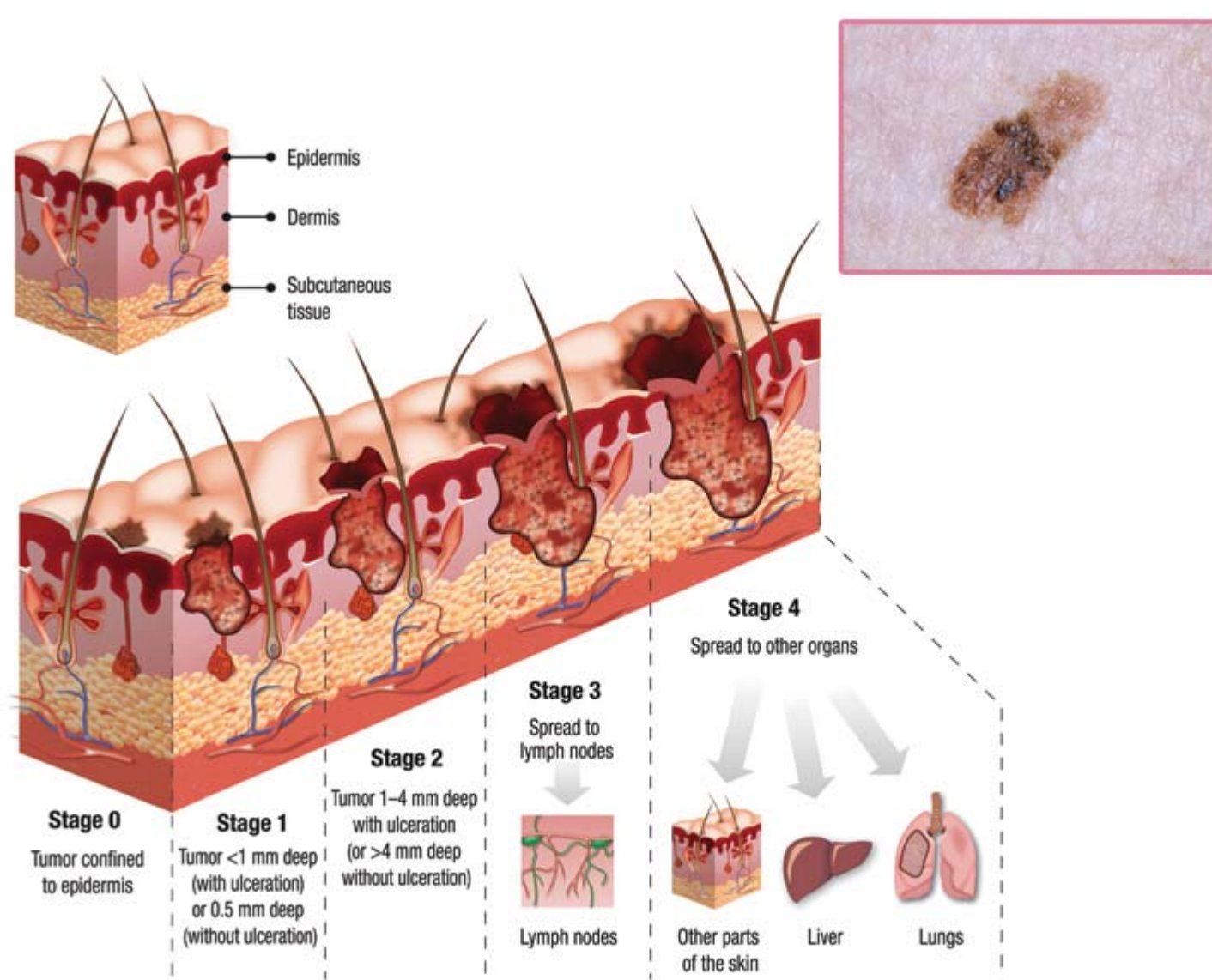


Fig. 1. Graphical representation of melanoma tumour progression. (<http://dyersburgskinandallergyclinic.com>)

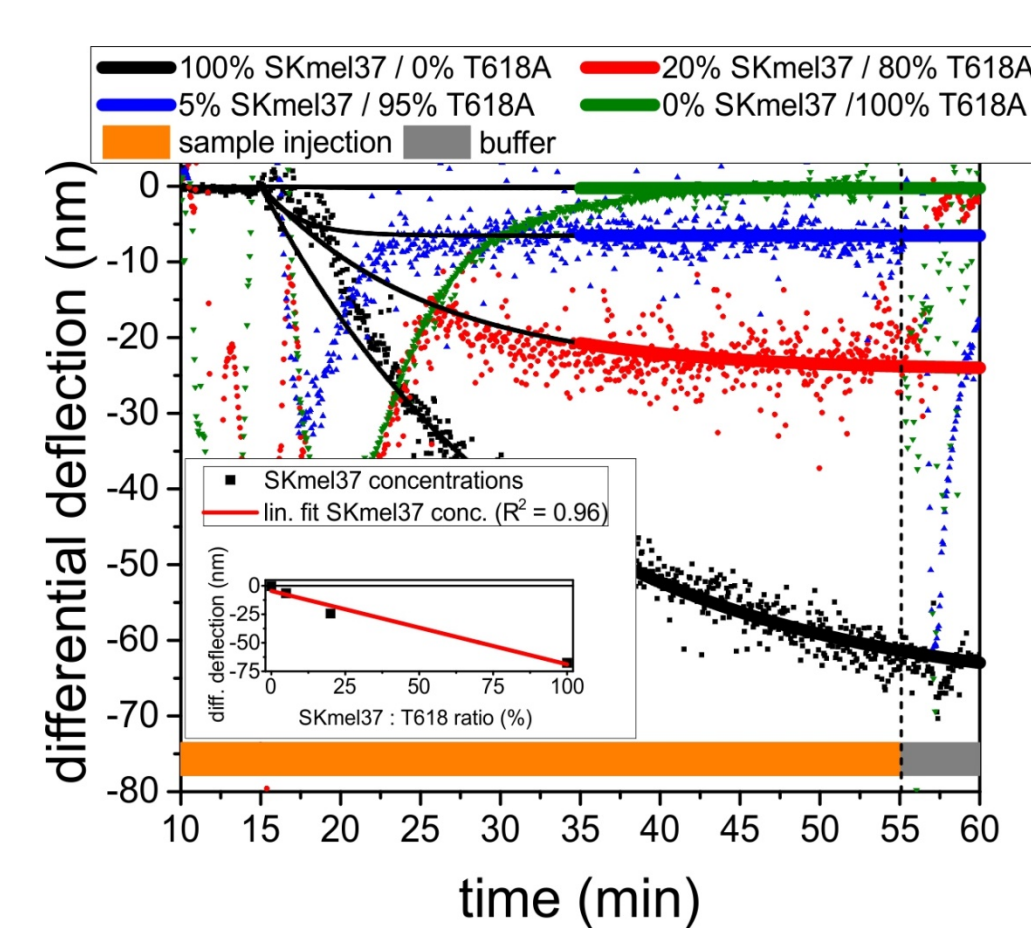
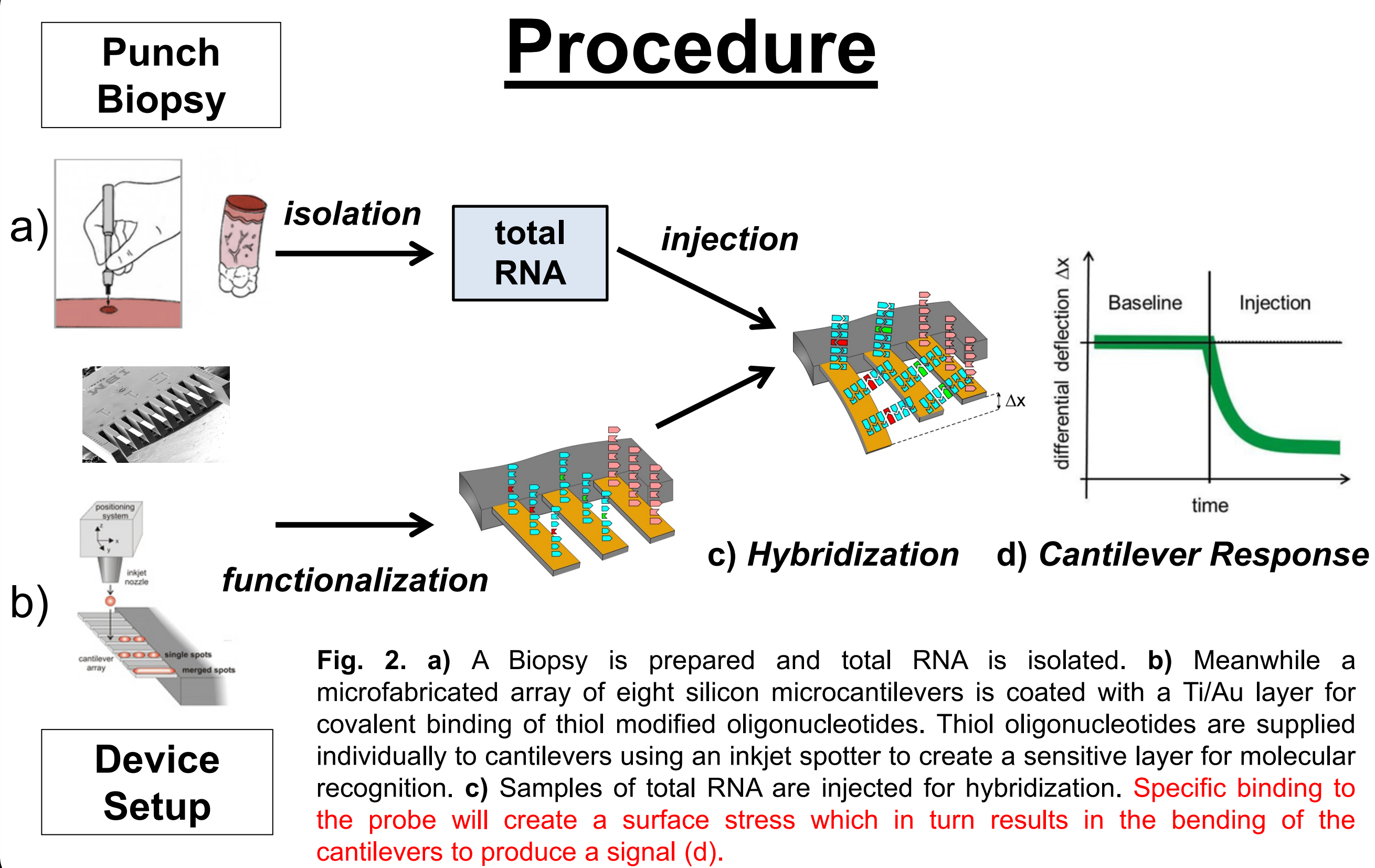


Fig. 3. Estimating detection limit for *BRAF*^{V600E} using RNA from cell lines: Different amounts of SK-Mel-37 *BRAF*^{V600E} positive total RNA are diluted with T618A *BRAF*^{V600E} negative total RNA to yield different ratios; 0%, 5%, 20% and 100% SK-Mel-37 content. Langmuir fits ($R^2 > 0.95$) are superimposed on top of the data. In the first 20 minutes after injection peaks occur originating from refractive index changes due to mixing effects. The fits were calculated based on data for the last 20 minutes only, before flushing with buffer, but the whole Langmuir fits are shown, with the initial 20 minutes in black. The inset shows the linear dependence ($R^2 = 0.96$) of the extrapolated differential deflections on the SK-Mel-37 concentration.

Results 1

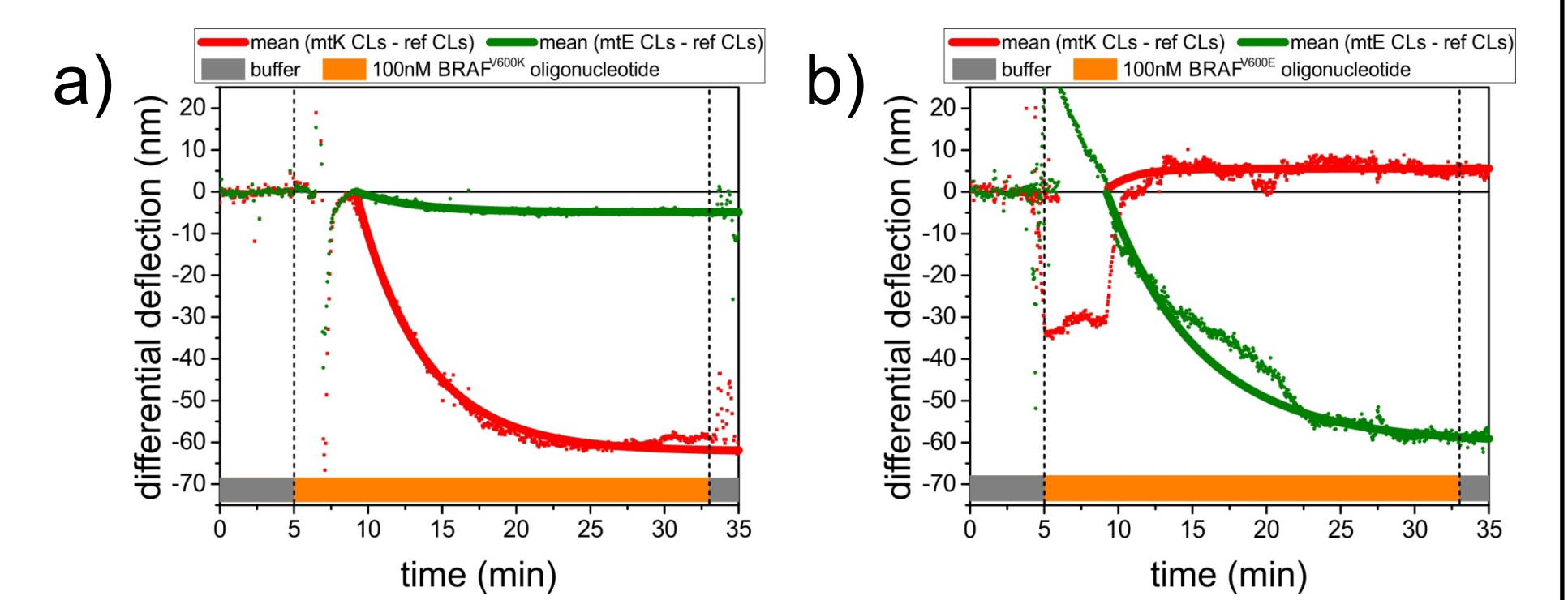


Fig. 4. *BRAF*^{V600E} is not the only relevant mutation for melanoma: *BRAF*^{V600K} is another recurrent albeit less frequent mutation present in 10% of cases. Using *BRAF*^{V600K} oligonucleotide targets we were able to discriminate between the *BRAF*^{V600E} and *BRAF*^{V600K} mutations. a) We observe that by injecting *BRAF*^{V600K} complement only the corresponding cantilevers are bending. b) In the analogous experiment using *BRAF*^{V600E} complement only the *BRAF*^{V600E} cantilevers are bending, demonstrating that we can distinguish two different mutations. Because of the array format, the analysis can be paralleled, so that the presence of multiple mutations could be simultaneously interrogated, allowing for an efficient analysis of targetable mutations in one assay.

Results 2

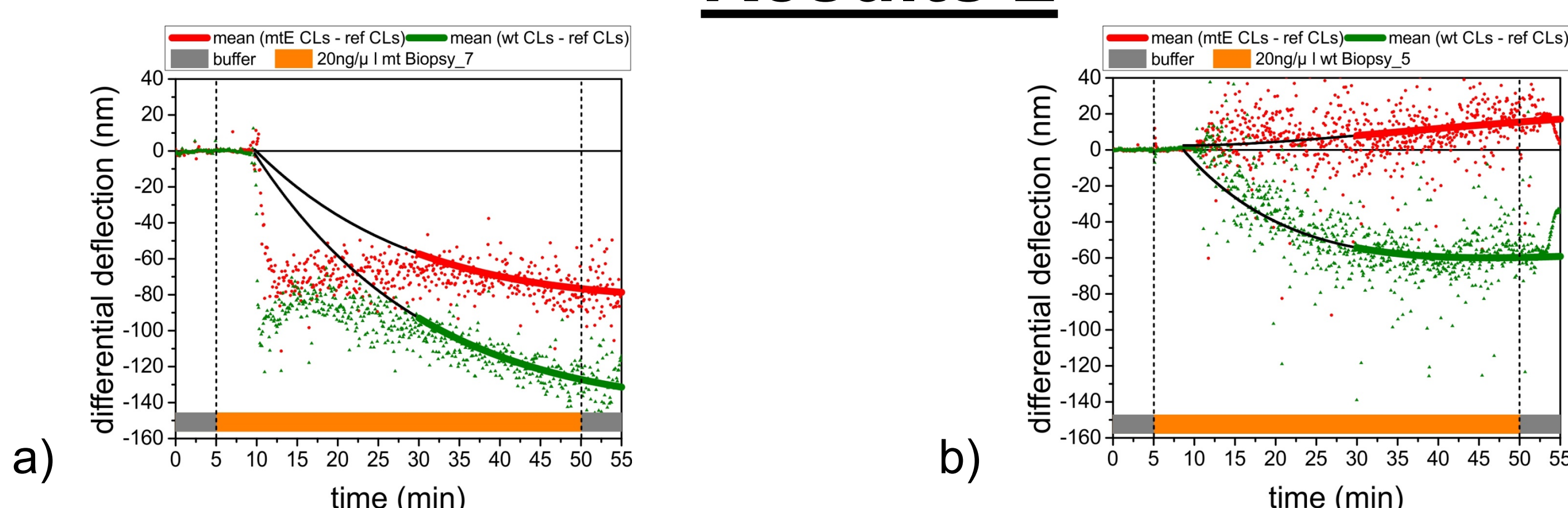


Fig. 5. Analysis of RNA samples from two biopsies. Differential signals between mutant probe (mt) and polyAC reference cantilever (ref) shown in red is shown as well as a combination of wt reference and polyAC reference cantilevers indicated by the green curve. a) Analysis of total RNA from *BRAF*^{V600E} positive Biopsy_7. b) Analysis of total RNA from *BRAF*^{V600E} negative Biopsy_5 (for biopsy numbers and origin see Table 1). Langmuir fits ($R^2 > 0.95$) are superimposed on top of the data. Since the first 20 minutes show injection peaks originating from refractive index changes due to mixing effects and the fits were calculated only for the last 20 minutes before flushing with buffer, but the whole Langmuir fits are shown including the initial 20 minutes in black.

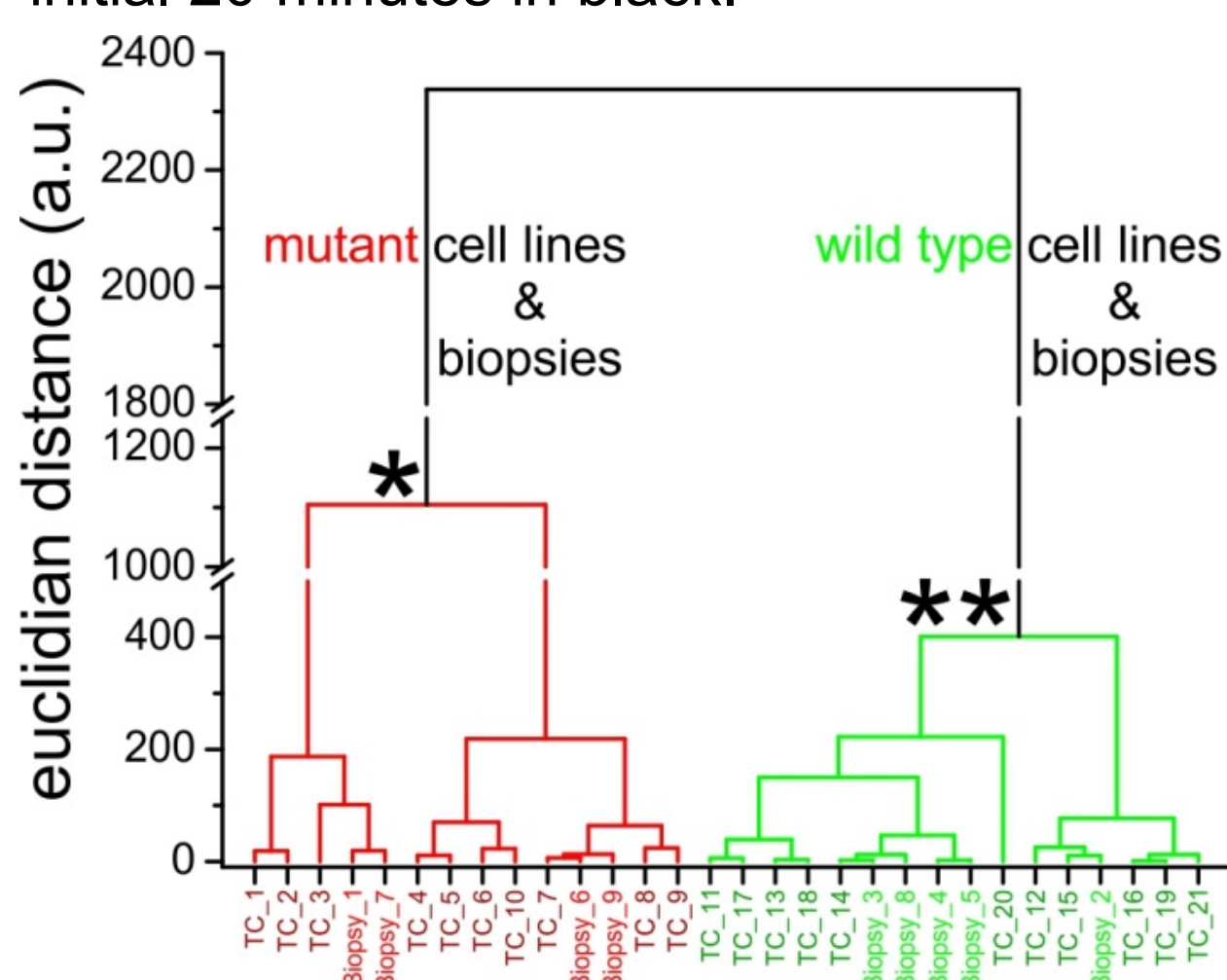


Fig. 6. Dendrogram of hierarchical cluster analysis including 10 *BRAF*^{V600E} positive (red branches, TC_1 – TC_10), 11 *BRAF*^{V600E} negative (green branches, TC_11 – TC_21) tissue culture samples and 9 biopsies (Biopsy_1 – Biopsy_9). Bifurcation points are indicated by (*) and (**). The *BRAF*^{V600E} positive biopsies 1, 6, 7, and 9 are indicated in bold red and the *BRAF*^{V600E} negative 2, 3, 4, 5, and 8 biopsies are depicted in bold green. The Euclidian distances are calculated using the method of sum of distances.

Conclusions

Number	Type of Biopsy	Origin	RNA yield. (µg)	RNA conc. (ng/µl)	BRAF Status Pathology	BRAF Evaluation Cantilever	% tumor cells as determined in pathology
Biopsy_1	FFPE	Lung metastasis	9.4	188	Mutant	Mutant	95%
Biopsy_2	Frozen	Mesenteric metastasis	48.45	969	Wild Type	Wild Type	90%
Biopsy_3	FFPE	Mesenteric metastasis	78.15	1563	Wild Type	Wild Type	not done
Biopsy_4	Frozen	Axillary lymph node metastasis	11.7	234	Wild Type	Wild Type	whole slide: 50%; marked area: 95%
Biopsy_5	FFPE	Axillary lymph node metastasis	417	8340	Wild Type	Wild Type	not done
Biopsy_6	FFPE	Cutaneous metastasis	626.95	12539	Mutant	Mutant	whole slide: 95%; marked area: 98%
Biopsy_7	FFPE	Lymph node metastasis	94.2	1885	Mutant	Mutant	marked area: 98%
Biopsy_8	FFPE	Axillary lymph node metastasis	133.2	2666	Wild Type	Wild Type	marked area: 98%
Biopsy_9	FFPE	Pleural metastasis	39.5	792	Mutant	Mutant	marked area: 98%

Table 1 shows the summary of a clinical study with nine samples of different origin, *BRAF*^{V600E} positive (**Mutant**) and negative (**Wild Type**) patients. Total RNA was extracted from either frozen (Frozen) or formalin-fixed paraffin-embedded tissue (FFPE) resulting in a range of different concentrations.

-The work shows that nanomechanical microcantilevers are able to identify mutations in complex samples ranging from cell lines to biopsies of patients.

-The technology is able to detect different mutations (*BRAF*^{V600E}, *BRAF*^{V600K}) that are relevant for malignant melanoma treatment.

-We successfully concluded the first pilot clinical study using nanomechanical microcantilevers.